

Jets and Jet-like Correlations at RHIC

Helen Caines

Department of Physics, Yale University, New Haven, CT, USA

I present an overview of some of the recent results on jets and jet-like correlation measurements from the Relativistic Heavy-Ion Collider (RHIC) at Brookhaven National Laboratory.

Jets are produced in the initial hard scatterings of an event and can therefore be exploited as probes of the hot and dense medium produced in heavy-ion collisions. Previous RHIC results indicate that this medium, the Quark Gluon Plasma (sQGP), is strongly coupled, with partonic degrees of freedom. High p_T colored partons passing through the sQGP are therefore believed to suffer energy loss via induced gluon radiation and elastic collisions, before exiting the medium and fragmenting in vacuum. Jet reconstruction and high p_T correlation studies allow us to investigate how the partons interact with the medium and how the medium responds to the partons moving through it. By comparing measurements from pp and d -Au to those in Au-Au collisions at $\sqrt{s_{NN}} = 200$ GeV we aim to disentangle cold nuclear matter effects from those of the hot and dense sQGP.

I. INTRODUCTION

Over the past decade the RHIC experiments have produced significant evidence that a Quark Gluon Plasma (sQGP) is being produced in ultra-relativistic heavy-ion collisions. This sQGP is strongly coupled and has partonic degrees of freedom. Hard probes are now being used to study how partons interact with the medium, and how the sQGP responds to energy deposited by these highly energetic partons as they travel through it. The results from Au-Au collisions are compared to those from pp and d -Au collisions where no QGP is believed to be created.

Jet quenching, the loss of energy of hard scattered partons to the medium, was first observed at RHIC via the single particles nuclear modification factor, R_{AA} [1]. The nuclear modification factor is defined as the ratio of Au-Au p_T spectrum normalized to the number of binary collisions (N_{bin}) to that of the pp data measured at the same collision energy. The R_{AA} of high p_T particles in central Au-Au indicated a suppression of up to a factor of 5 [1], while photons, colorless objects, reveal an $R_{AA} = 1$ [2]. These results suggest that the suppression is due to partons interacting with, and hence losing energy to, the hot and dense colored medium. R_{AA} measures however have a couple of limitations. First it is not possible to infer the initial partonic energy from the final state hadron. Second surface emission leads to an inherent insensitivity to the medium's density; no matter how dense the medium those partons near the surface will always escape and be detected [3].

To attempt to alleviate both these issues the collaborations are now performing full jet reconstruction. An added advantage is that by studying the fragmentation patterns we can hope determine not only how much energy is lost from the initial parton but also how the energy is redistributed. Both STAR and PHENIX use jet finding algorithms from the FastJet package [4], in addition PHEINX uses a Gaussian filter code, details of which can be found here [5] and STAR has used a traditional mid-point cone algorithm [6].

Neither RHIC experiment has hadronic calorimetry included in their detector designs, hence the full jet energy is not directly accessible but is assessed by combining charged particle momenta via tracking devices with neutral energy measurements from electro-magnetic calorimetry. In addition the energy from long-lived neutral hadrons, such as the neutron and K_L^0 is missed. This leads to a significant difference in the jet energy reconstructed and that of the initial, so-called particle level jet. This difference, as well as the jet energy resolution, has to be evaluated and corrected for before final results can be presented. For instance, the detector performances have been evaluated via simulations by STAR and show that the jet energy resolution in pp data varies from 10-25%, for 40-10 GeV/ c jets [7].

II. JETS IN PP AND D-AU COLLISIONS

For pp collisions the reconstructed raw jet spectra reconstructed with the Anti- K_T , K_T and SIScone algorithms were the same within 10%, confirming that they have similar behaviours in this low multiplicity data, Fig. ref-Fig:JetCompare [7]. The inclusive jet, Fig. 2, and di-jet cross-sections, Fig. 3, have been measured by STAR using the increased statistics of the 2006 data [8]. A midpoint cone algorithm [6] with a cone radius of 0.7, a split-merge fraction 0.5 and a seed energy of 0.5 GeV was used. When hadronization and underlying event uncertainties are included both sets of data are well described by NLO theory [9, 10].

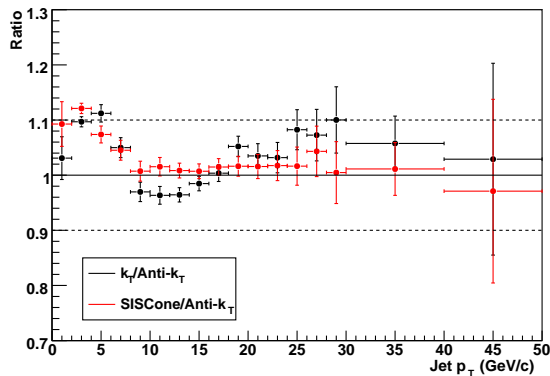


FIG. 1: The ratio of reconstructed jets for various FastJet algorithms, $K_T/Anti-K_T$ and $SIS\text{Cone}/Anti-K_T$ as a function of reconstructed jet p_T .

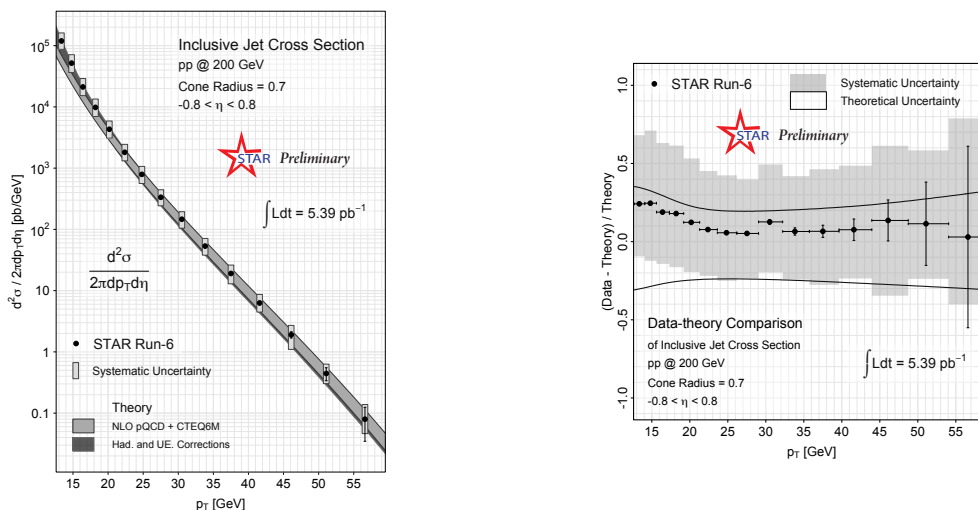


FIG. 2: Left: The 2006 measured inclusive jet cross section for pp collisions at $\sqrt{s_{NN}}=200$ GeV. Right: (Data-Theory)/Theory.

The measured fragmentation functions of both STAR [11] and PHEINX [12] agree, within errors, with PYTHIA simulations [13], see Fig. 4. The PHENIX data use the Gaussian filter with a width of 0.3, and are fully corrected. While the data from STAR are not yet corrected to the particle level and are therefore compared to PYTHIA 6.410 [13], tuned to the CDF 1.96 TeV data (Tune A), predictions passed through STAR's simulations and reconstruction algorithms. The agreement with PYTHIA simulations even for $R=0.7$ suggests that there are only minor NLO contributions beyond those mimicked in the PYTHIA parton-shower calculations at RHIC energies.

We also investigate jet production in d -Au collisions, where cold nuclear matter effects are expected to be present but no QGP formed. For example, the presence of the Au nucleus may induce additional initial and final state radiation, or result in scatterings of fragmentation particles as they escape the nucleus. The measured d -Au mid-rapidity jet nuclear modification factor, R_{CP} , where peripheral d -Au events are used instead of pp data, is shown from PHENIX in Fig. 5 left panel, for three different centrality bins. Here the Anti- K_T algorithm with $R=0.3$ was used. A slight modification of the jet spectrum is observed in d -Au collisions, with the central d -Au jet cross-section showing the greatest suppression. These results are consistent with the π^0 results and are likely an indication of cold nuclear matter effects such as modifications of the nuclear PDFs and/or energy loss in the cold matter. Since these effects may result in more subtle modifications than that of the overall jet yields, another way to probe for these cold nuclear matter effects is via di-jet correlations. Re-scatterings in the nucleus may result in a broadening of the di-jet $\Delta\phi$ distribution. The mean transverse momentum of the fragmentation

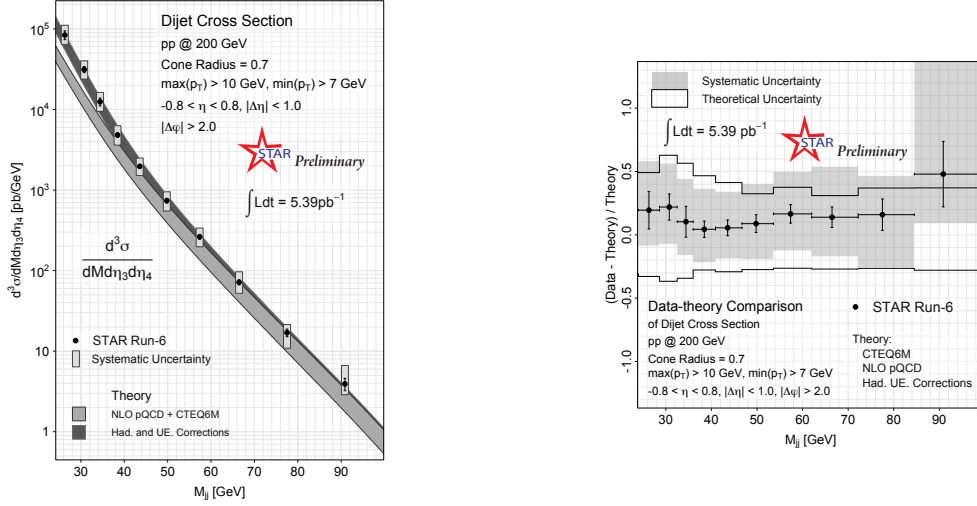


FIG. 3: Left: The 2006 measured inclusive di-jet cross section for pp collisions at $\sqrt{s_{NN}}=200$ GeV. Right: (Data-Theory)/Theory.

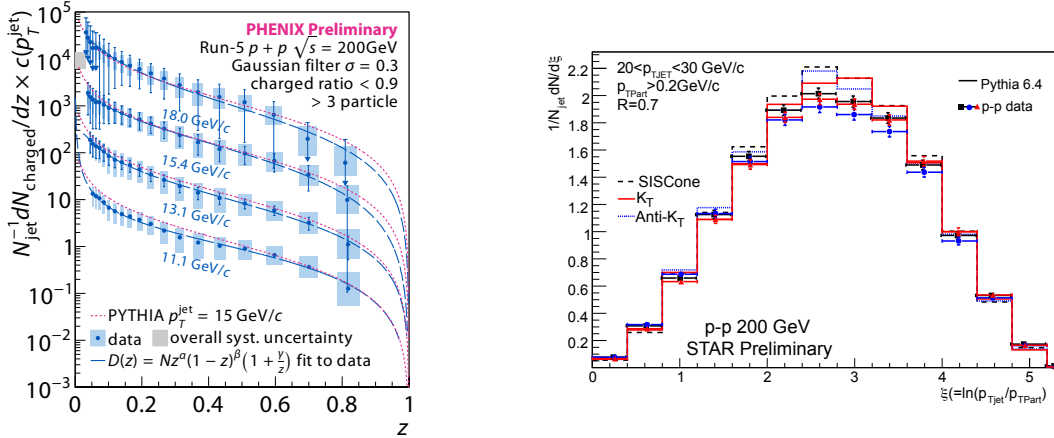


FIG. 4: Left: PHENIX Run-5 pp charged particle (electrons rejected) fragmentation function as a function z ($=p_{hadron}/p_{jet}$). A vertical scaling of $c(p_T^{jet}) = 10^k, k = 0, \dots, 3$ is applied. The shaded boxes indicate systematic uncertainties, and error bars indicate statistical uncertainties. From [12]. Right: Jet FF as a function ξ from STAR using the K_T , Anti- K_T and SIScone algorithms for $R=0.7$. The curves are the PYHTIA predictions.

products with respect to the jet axis, $\langle j_T \rangle$, and the mean transverse momentum kick given to di-jet pair, $\langle k_T \rangle$, are two variables used for these investigations. The $\langle j_T \rangle$ was measured via di-hadron correlations and found to be constant at ≈ 0.55 GeV/c for all p_T triggers measured and for both pp and d -Au events at $\sqrt{s_{NN}}=200$ GeV [15]. However, as shown in Figure 5 right panel the $\langle k_T \rangle$ is systematically higher for the d -Au data than for the pp data for all p_T jet and p_T trigger ranges measured. This suggests that while cold nuclear matter effects are small they still result in a minor deflection/broadening of partonic trajectories, the fragmentation appears to be unaffected.

The underlying event (UE) is an important element of hadronic collisions and is defined as those particles not produced in the initial hard scatterings. Hence it includes beam-beam remnants, particles from initial and final state re-scatterings and those resulting from soft or semi-hard multi-parton interactions, pile-up is not included in the UE definition and must be removed. In pp events at RHIC the UE is small and is often neglected, however in d -Au collisions it becomes sizable. CDF initiated such an analysis [16]. First the jets are reconstructed, next each event is split into four sections defined by their azimuthal angle with respect to the leading jet axis ($\Delta\phi$). The range within $|\Delta\phi| < 60^\circ$ is the lead jet region and an away jet area is designated for $|\Delta\phi| > 120^\circ$. This leaves two transverse sectors of $60^\circ < |\Delta\phi| < 120^\circ$ and $120^\circ < \Delta\phi < -60^\circ$. One is called the TransMax region and is the

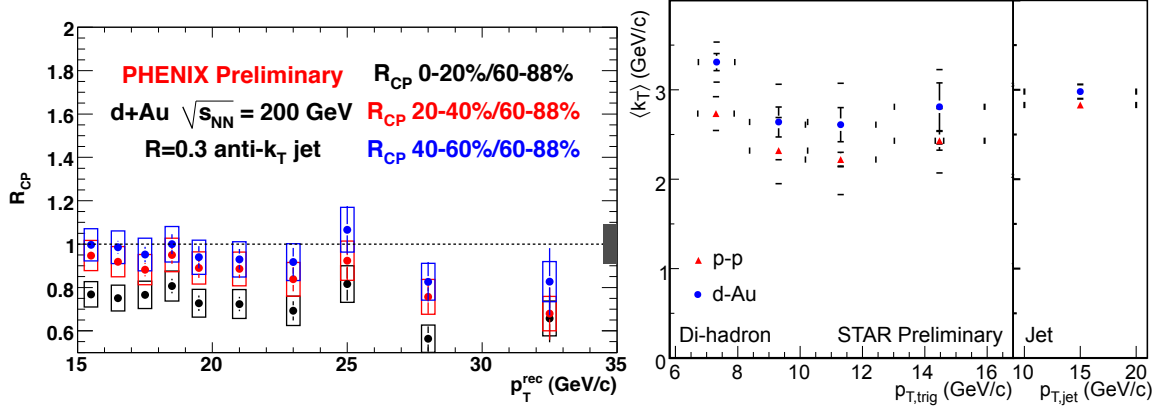


FIG. 5: Left : Jet R_{CP} for d-Au collisions for three different centrality selections. Right: The measured $\langle k_T \rangle$ for d-Au and pp data at $\sqrt{s_{NN}}=200$ GeV from di-hadron correlations and di-jet measurements from STAR. Vertical bars show the statistical and systematic uncertainties, horizontal bars indicate the bin widths.

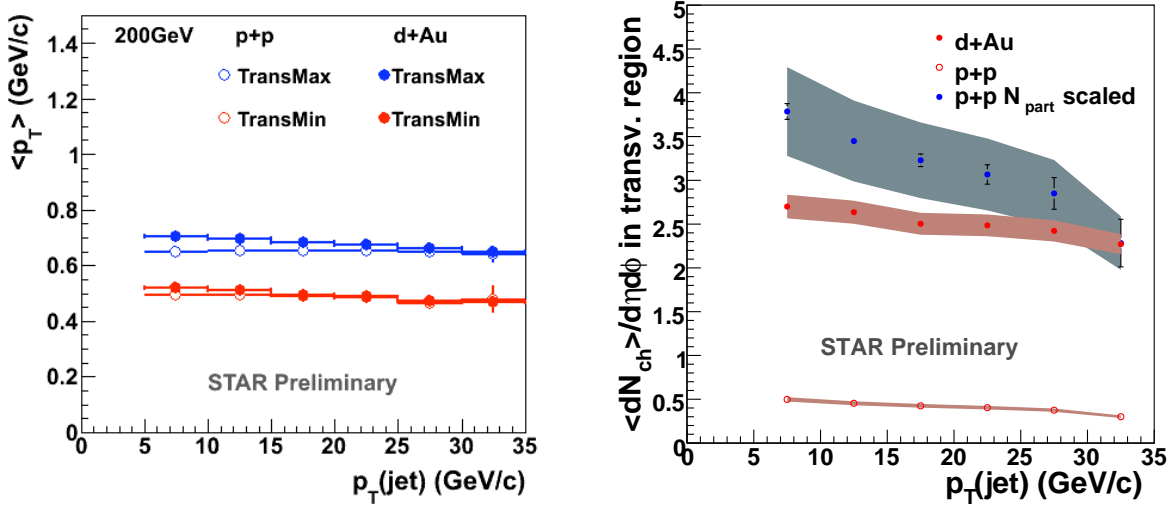


FIG. 6: Mean p_T (left) and mean number of charged particles per unit η and ϕ (right) in the transverse regions for pp and d-Au collisions. All data are from $\sqrt{s_{NN}}=200$ GeV.

transverse sector containing the largest charged particle multiplicity. The second sector is termed the TransMin region. Two sets analyses can then performed, a “leading” jet study, where at least one jet is found in STAR’s acceptance, and a “back-to-back” study which is a sub-set of the “leading” jet collection. This sub-set of events has two (and only two) found jets with $p_T^{awayjet}/p_T^{leadjet} > 0.7$ and $|\Delta\phi_{jet}| > 150^\circ$, this selection suppresses hard initial and final state radiation of the scattered parton. The TransMax region has an enhanced probability of containing contributions from these hard initial and final state radiation components. Thus, by comparing the TransMax and TransMin regions in the “leading” and “back-to-back” sets we can extract information about the various components in the UE. The properties of the UE in both pp and d-Au events are being studied, this is the first time such an analysis has been undertaken for d-Au collisions. Since this study is preformed at mid-rapidity it is likely that there is little to no contribution from the beam-beam remnants. Both the number of particles in and the momentum distribution of the underlying event appear to be largely independent of the leading jet’s p_T in both pp and d-Au collisions, Fig. 6. The mean transverse momentum is similar for pp and d-Au events in both the TransMax and TransMin regions as can be seen in Fig. 6 left panel. Meanwhile the average number of charged particles per unit η and ϕ increases by \sim factor 5 from pp and d-Au collisions, right panel of Fig. 6. This increase in particle production is only slightly less than N_{part} scaling of the pp

data would predict, also shown in figure 6. All the results are the same within errors for the “leading” and “Back-to-Back” data sets [17, 18], which suggests that the hard scattered partons emit very small amounts of large angle initial/final state radiation at RHIC energies.

III. JETS IN HEAVY-ION COLLISIONS

The presence of jets in heavy-ion events is clearly evident in Fig. 7, despite the significant underlying event. The left panel shows a di-jet event in the PHENIX detector from a $\sim 20\%$ central Cu-Cu collision as found by the Gaussian filter algorithm [19]. The right panel shows a central Au-Au event in the STAR detector. Each grid cell indicates the summed p_T of the charged tracks reconstructed in the TPC and neutral energy recorded in the electro-magnetic calorimeter.

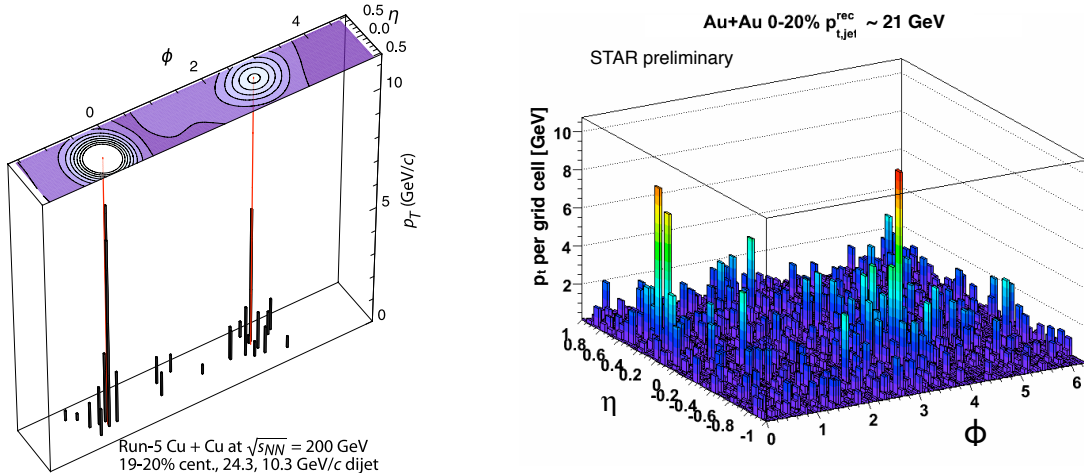


FIG. 7: Di-jets in heavy-ion events at $\sqrt{s_{NN}} = 200$ GeV Left: PHENIX Run-5 Cu-Cu $\sim 20\%$ centrality. Charged tracks and photons are shown at the bottom by a lego plot. The distribution of the Gaussian filter output values of the event is shown at the top as a contour plot. The maxima in the filter density are reconstructed as jet axes, shown as red lines at the positions on the contour and Lego plots. Right: STAR central Au-Au event, the summed p_T of charged tracks and electro-magnetic calorimeter towers per grid cell are shown. Clear di-jet peaks emerge above the background.

In order to extract information regarding jets and the interactions of hard scattered partons with the sQGP it is essential to first understand the enormous background the jet is immersed in and its fluctuations. This background is predominantly formed from the soft underlying bulk particle production and is thus strongly dependent on the centrality of the collision. Schematically, assuming all the initial partonic energy is recovered by the jet finders the measured jet spectrum in Au-Au collisions is:

$$\frac{d\sigma_{AA}}{dp_T} = \frac{d\sigma_{AA}}{dp_T} \otimes F(A, p_T) \quad (1)$$

where $F(A, p_T)$ accounts for the background and its fluctuations, which are a function of the jet area and the p_T of the reconstructed jet. Initially it was assumed that these fluctuations could be accounted for by a simple Gaussian ansatz, however more detailed studies have shown this modeling to be insufficient. If the background is due to independently emitted particles then in a fixed area the number fluctuations are well described by a Poisson distribution, while those of the mean p_T result in a Gamma distribution, assuming a fixed number of particles, M [21]. Therefore

$$F(A, p_T) = \text{Poisson}(M(A)) \otimes \Gamma(M(A)\langle p_T \rangle) \quad (2)$$

Such a modeling of $F(A, p_T)$ gives a good description of the the summed p_T in the random cones of area A on a toy simulation where particles with $dN/d\eta = 650$ are thrown with a $T=290$ MeV. The mean of the $F(A, p_T)$ distribution is given by ρA . ρ is the median $\{p_{T,i}^{jet, reco}/A_i\}$ in the event and $p_T^{jet, reco}$ is the reconstructed jet p_T : When however the FastJet jet finders are used, the description is not exact, suggesting that the jet finders clustering does not occur in a truly random fashion, as should be expected. To investigate the resilience of the

jet finding in heavy-ion events to these fluctuations we are using probe embedding into real Au-Au events. A particle, or jet, of a known transverse momentum, p_T^{embed} , is embedded into an event, the Anti- K_T algorithm run and the reconstructed jet containing the embedded probe identified. Then

$$\delta p_T = p_T^{jet, reco} - \rho \cdot A - p_T^{embed} \quad (3)$$

is calculated. The δp_T distributions are then calculated over many events for different embedded objects. Single pions, PYTHIA jets, and qPYTHIA jets (where the fragmentation pattern is altered from that of vacuum fragmentation) [22] have been used as well as various p_T^{embed} . Figure 8 left panel shows the resulting δp_T distribution for a single 30 GeV/c pion embedded into a 0-20% central Au-Au event [23]. The right panel of Fig. 8 shows the distribution of the event-wise difference

$$\Delta \delta p_T = \delta p_T^\pi - \delta p_T^{jet}, \quad (4)$$

between δp_T for a PYTHIA-generated jet with $p_T > 30$ GeV/c probe and that of a pion with the same p_T , η , and ϕ . Similar results are seen when qPYHTIA jets are used and for lower p_T probes. This study reveals the Anti- K_T response is insensitive to the fragmentation pattern of the probe, greater than 70% of the time $|\Delta \delta p_T| < 200$ MeV/c. This is a crucial property for the jet finder used in heavy-ion jet quenching studies since we do not yet have a complete description of the fragmentation functions of partons which traverse the sQGP. Also importantly the Anti- K_T algorithm has been shown to respond in a predominantly geometric fashion and hence is fairly impervious to back-reaction effects [24].

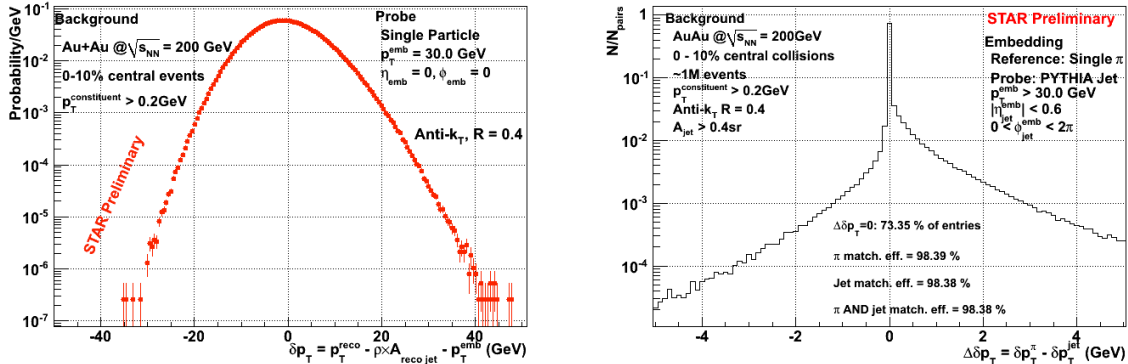


FIG. 8: Left: δp_T distribution for a single pion with $p_T = 30$ GeV/c embedded into a 0-20% central Au-Au event. Right: The event-by-event difference in δp_T for a PYTHIA embedded jet, $p_T > 30$ GeV/c, and a single pion with same p_T , η and ϕ as the jet.

For unbiased jet reconstruction one would expect the jet R_{AA} to be close to unity, possible deviations might occur due to initial state effects in the Au-Au collisions. However, the left panel of Fig. 9 shows that even for $R=0.4$ the jet R_{AA} is likely below unity, due to the large systematic errors the results are just compatible with unity [25]. The jet R_{AA} is however significantly above that of single hadrons with $p_T > 20$ GeV/c ($R_{AA}^{hadron} \approx 0.2$). One can also observe that there are significant differences between the results for the K_T and Anti- K_T algorithms which is expected given their different responses to the heavy-ion background. The ratio of the number of reconstructed jets for $R=0.2$ compared to $R=0.4$ is less for Au-Au data than for pp right panel of Fig. 9 [25]. Taking these two results together we conclude that the jet algorithms do not recover as much of the original partonic energy in Au-Au events as the same algorithms and settings run on pp data. Further, Fig. 9 indicates that this is likely due to the fact that particles are emitted at larger cone angles in Au-Au events compared to pp events with the same jet energy, with considerable energy, even at higher jet p_T outside of $R=0.4$.

Di-jet coincidence rate measurements provide us with evidence that there is a path-length dependence to the partonic energy loss. In this analysis “trigger” jets are identified which have a reconstructed jet $p_T > 20$ GeV/c when only particles with $p_T > 2$ GeV/c are considered by the Anti- K_T algorithm. These trigger jets also contain a barrel electro-magnetic calorimeter tower with $E_{tow} > 5.4$ GeV/c. This high z fragmentation requirement biases the trigger jet to being preferentially emitted from the surface of the medium and/or to have only minimally interacted with the medium. Such a surface bias in turn maximizes the average distance traversed by the recoil jet through the medium. If partonic energy loss is dependent on the path-length through the medium, the recoil jet will therefore reveal a greater suppression than that observed for the unbiased jet

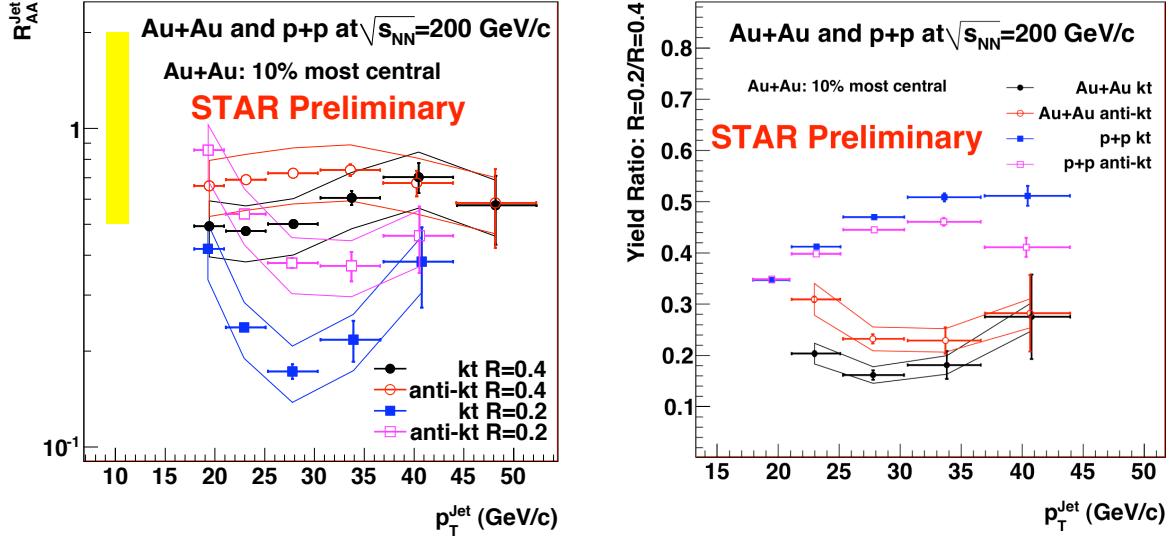


FIG. 9: Left: Jet R_{AA} . Right: The ratio of the number jets found with $R=0.2$ to those found with $R=0.4$ for pp and Au-Au events as a function of jet p_T .

population. The relative probability of reconstructing a di-jet pair in Au-Au is compared to that in pp is shown in Fig. 10. This relative probability is suppressed by an approximate factor of 5 [26], i.e. a much stronger rate of suppression than observed for the inclusive jets. This results supports the notion of a path length dependent energy loss term.

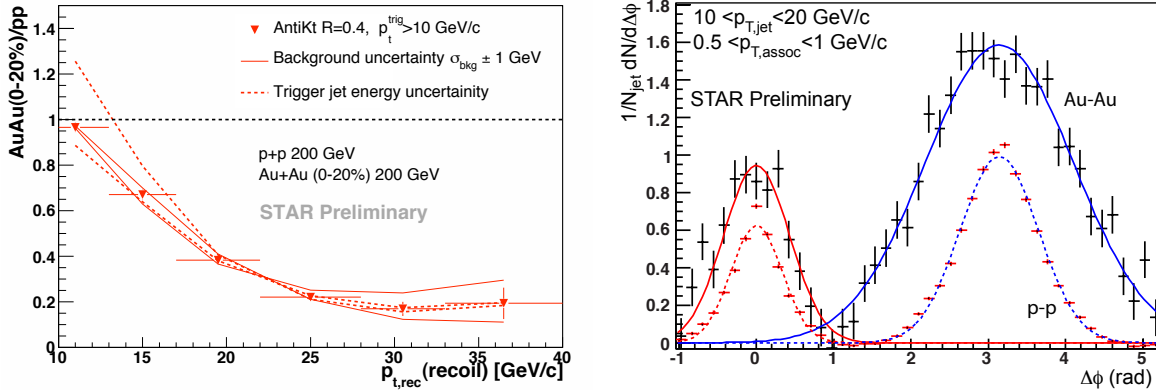


FIG. 10: Left: Di-jet reconstruction probability in Au-Au over pp for $R=0.4$ using the Anti- K_T algorithm. The curves indicate the systematic uncertainties in the estimation of the background fluctuations (solid) and of the p_T of the trigger jet assuming a jet resolution of 25% (dotted). Right: Jet-hadron correlations for $0.5 < p_T^{\text{assoc}} < 1$ GeV/c for pp and Au-Au collisions.

To investigate further the jet broadening and softening indicated by the studies mentioned above we turn to jet-hadron correlations. In this analysis a “trigger” jet (defined as in the di-jet analysis above) is used to determine the jet axis and the $\Delta\phi$ correlation of *all* charged particles in the event relative to this axis is examined, for more details on this analysis see [28]. An example of such a correlation is shown in Fig. 10 right panel, again a softening and broadening of the distributions of particles from jets is indicated for low p_T associated. The per trigger $\Delta\phi$ distributions for pp and Au-Au event, plotted as a function of the associated charged particle p_T , are summarized in Figures 11 and 12. The Gaussian widths of the away-side correlations in pp and Au-Au are shown in Fig. 11. The Au-Au distributions are broader than those in pp for low p_T associated particles, accompanied by an significant increase in the low p_T associated yields [28]. For high p_T associated particles the Au-Au recoil jet correlation width is equivalent to that of pp but there is a significant reduction in the particle yield. Re-scattering of the initial parton could also potentially cause such a broadening rather than a modification of the fragmentation. Therefore the di-jet $\Delta\phi$ distributions in pp and Au-Au data,

PYTHIA events, and PYTHIA jets embedded into Au-Au events were studied. The results are shown in right plot of figure 11. The distribution is broader for the Au-Au data, however much of this broadening can be attributed to de-resolution of the jet axis due to the large underlying event, as a similar broadening is also observed in the PYTHIA+Au-Au event data. A similar result has been reported by PHENIX, who show that the $\Delta\phi$ distributions of di-jet events in Cu-Cu collisions do not vary as a function of centrality [27]. The red curve in the left plot of Fig. 11 indicates the expected width of the away-side $\Delta\phi$ distribution if the Au-Au fragmentation was pp like, but with the jet axis direction smeared to reproduced the width of the $\Delta\phi$ Au-Au di-jet data. Clearly such a smearing cannot fully explain the observed broadening, and it also does not explain the enhanced low p_T yields.

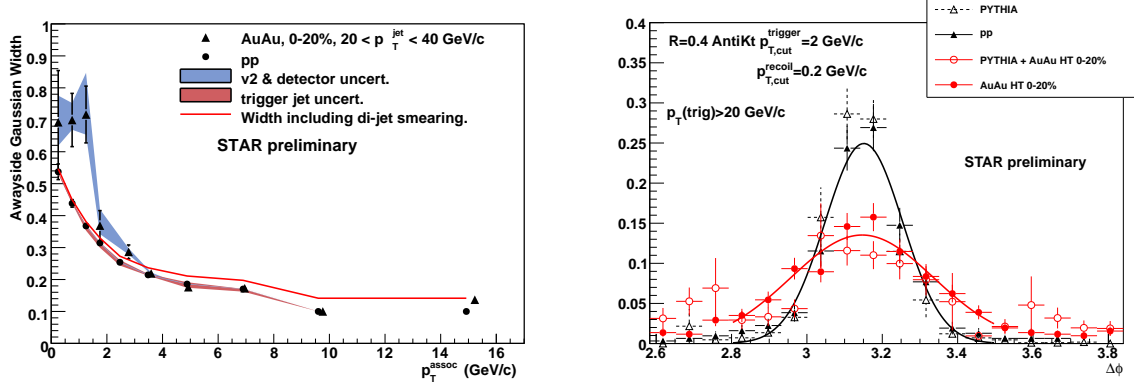


FIG. 11: Left: The Gaussian widths of the away-side correlations as a function of p_T^{assoc} . Right: Di-jet $\Delta\phi$ distributions for various data sets at $\sqrt{s_{NN}}=200$ GeV collisions. Solid curves are Gaussian fits to the data.

The integrated yield difference, ($D_{AA} = Yield_{AA} \times \langle p_T^{assoc} \rangle - Yield_{pp} \times \langle p_T^{assoc} \rangle$) of the near- and away-side correlations as a function of p_T^{assoc} are plotted in Fig. 12. As expected, the ‘‘surface’’ bias of the trigger causes the near-side D_{AA} to be consistent with zero for all p_T^{assoc} . This means that there is an approximate energy balance, and a similarity of the associated p_T particle distributions for Au-Au and pp data for the trigger jet. The away-side data, Fig. 12 right panel, reveals that the low p_T hadron enhancement in the Au-Au data is approximately matched by the high p_T associated particle suppression. This suggests that the broadening and softening observed in the away-side correlation data is indeed due to a modification of the partonic fragmentation and not from residual soft background particles.

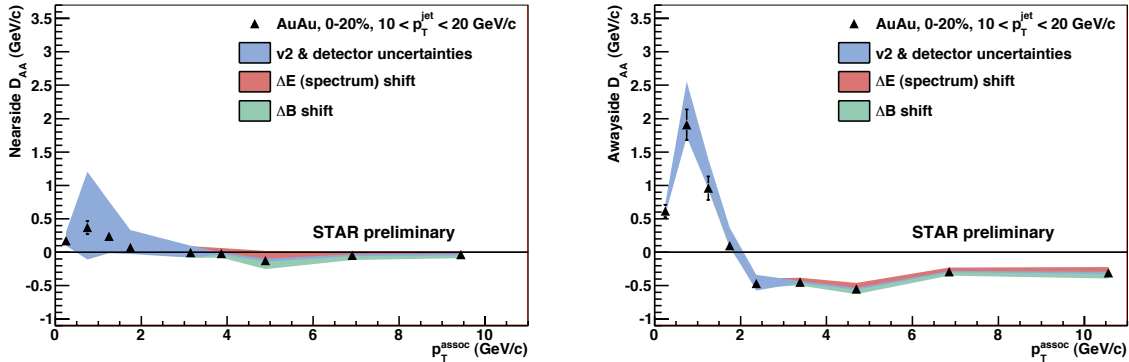


FIG. 12: Jet-hadron D_{AA} distributions for the near-side (left) and away-side (right). For details on the systematic uncertainty bands see [28].

To remove the surface bias of the trigger object introduced in the di-jet and jet-hadron analyses discussed above PHENIX have been investigating γ -hadron correlations. Direct photon-hadron correlations are an ideal channel for studying energy loss since direct photons do not interact via the strong force and hence traverse the sQGP unmodified. At leading order pQCD, direct photons are produced from a Compton scattering of $q + g \rightarrow q + \gamma$ or quark annihilation $q + \bar{q} \rightarrow g + \gamma$. To conserve energy and momentum a matching recoil

jet is also produced. The energy of the photon can then be used as a proxy for the jets initial energy and the fragmentation function of the recoil jet can be calculated. γ -hadron $\Delta\phi$ correlations have been measured in both pp and Au-Au collisions [29], an isolation cut is used around the trigger photon to reduce contamination from π^0 and fragmentation photons. A fragmentation function is then deduced for the recoil jet correlation at $|\Delta\phi - \pi| \leq \pi/2$. The resulting distributions as a function of $\xi = -\ln(x_E)$ where $x_E = p_T^{\text{hadron}} \cos(\Delta\phi) / p_T^{\text{photon}}$ are shown in Fig. 13 for pp and central Au-Au collisions. The preliminary Au-Au and published pp data are plotted and compared to the TASSO measurement [30] and a Modified Leading Logarithmic Approximation (MLLA) in medium prediction [31]. The TASSO data and MLLA curve have been arbitrarily scaled down by a factor of ten to account for the limited PHENIX η acceptance as in [32]. The shape of the isolated pp data are in good agreement with the TASSO measurement of the quark fragmentation function from $e^+ + e^-$ collisions. The Au-Au results show depletion at low ξ and possible enhancement at high ξ compared to the pp data. These results again indicate that the energy lost by high p_T partons reappears as soft hadrons correlated with the initial parton's path.

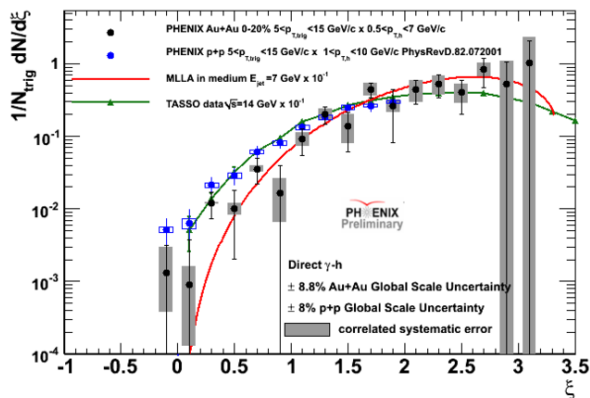


FIG. 13: ξ distributions from PHENIX γ -hadron correlations in Au-Au data (black circles) and pp data (open blue circles) compared to TASSO data (green triangles) and MLLA in medium prediction (red curve).

IV. SUMMARY

In conclusion, both PHENIX and STAR are making quantitative steps in our understanding of jet production and fragmentation in pp , d -Au, and Au-Au collisions at RHIC at $\sqrt{s_{NN}} = 200$ GeV over a wide kinematic range.

Both the jet and di-jet cross-section in pp collisions are well described by next-to-leading order calculations once hadronization and the effects of the underlying event are taken into account. PYTHIA simulations reproduce the measured distributions of the fragmentation products even at large jet resolution parameters indications that NLO corrections, beyond those implemented in PYHTIA, are small.

Jet production in d -Au collisions is slightly suppressed, particularly in central d -Au events when compared to binary scaled pp or peripheral d -Au data. Together with the k_T and j_T measurements as a function of jet p_T this indicates that there are small cold nuclear matter effects present but that these do not affect the shape and distribution of the fragmentation particles produced.

Underlying event measurements of the pp and d -Au data show no significant changes as a function of jet p_T . The mean number of charged particles produced in the transverse region approximately scales with the number of participants in the event, while the mean p_T of these particles remains constant between pp and d -Au data.

Our understanding of the background, and most importantly its fluctuations, in heavy-ion events has significantly improved. The Gaussian ansatz of the fluctuations has been shown to be incorrect, they are more closely reproduced from a folding of a Gamma function with a Poisson that depend on the jet area, multiplicity of the background and its mean p_T . It has also been shown that the Anti- K_T algorithm's response to the background and its fluctuations is largely independent of the fragmentation pattern of the jet.

Using a jet resolution parameter of $R=0.4$ the measured jet cross-section in central Au-Au collisions does not binary scale compared to pp data, the jet $R_{AA} < 1$. This reveals that the lost partonic energy is spread to radii beyond $R=0.4$. Further the Au-Au $R=0.2/R=0.4$ ratio as a function of jet p_T is lower than that measured in pp showing this broadening is there for all radii. The di-jet reconstruction probability in Au-Au collisions is suppressed as would be expected if the partonic energy loss is pathlength dependent.

Both jet-hadron and direct photon-hadron correlations indicate an enhanced production of hadrons a low p_T compared to pp baseline measurements which appear to compensate the suppressed particle production at high p_T . However, the high p_T associated particles while suppressed in number compared to pp data do not reveal any broadening in the jet-hadron correlations. This is in agreement with a scenario where the scattered parton loses energy in the sQGP but then fragments outside of the medium as it would in vacuum albeit with a reduced energy. The di-jet $\Delta\phi$ distributions indicate no obvious deflection of the parton's path although significant path length dependent energy is lost as it traverses the medium.

All of the measurements made in heavy-ion collisions show that energy lost by high Q^2 scattered partons re-appears as soft particle production, with properties similar to that of the bulk, that remains largely correlated to the jet axis.

-
- [1] D. d'Enterria Nucl. Phys. A 827 356c (2009) and references therein.
 - [2] A. Adare *et al.* (PHENIX) Phys. Rev. Lett. 94, 232301 (2005).
 - [3] A. Dainese C. Loizides and G. Paic Eur. Phys. J C38 461 (2005). K.J. Eskola, H. Honkanen C.A. Salgado and U.A.. Wiedemann Nucl. Phys. A747 511 (2005).
 - [4] M. Cacciari and G. Salam, Phys. Lett. **B 641**, 57 (2006). M. Cacciari, G. Salem and G. Soyez, JHEP **0804**, 063 (2008). M. Cacciari and G. Salem, Phys. Lett. **B 659**, 119 (2008).
 - [5] Y.-s. Lai and B.A. Cole arXiv:0806.1499 (2008).
 - [6] G.C. Blazey *et al.* arXiv:hep-ex/0005012 (2000).
 - [7] H. Caines (for STAR) arXiv:1106.6247 (2011).
 - [8] T. Sakuma and M. Walker (for STAR) arXiv:1012.1173v1, T. Sakuma, Ph.D. Thesis, MIT (2010).
 - [9] B. Jäger, M. Stratmann, and W. Vogelsang, Phys. Rev. D **70**, 034010 (2004).
 - [10] J. Pumplin *et al.*, JHEP 07, 012 (2002).
 - [11] H. Caines (for STAR), Nucl. Phys. A830 (2009).
 - [12] Y.-s. Lia (for PHENIX) arXiv:1005.2801 (2010).
 - [13] T. Sjostrand, S. Mrenna, P. Skands JHEP **0605** 026, arXiv:hep-ph/0603175v2 (2006).
 - [14] M. Purschke (for PHENIX) to be published as QM2011 proceedings.
 - [15] M. Mondal (STAR), poster at QM2011, [https://indico.cern.ch/materialDisplay.py?contribId=231 &sessionId=65&materialId=poster&confId=30248](https://indico.cern.ch/materialDisplay.py?contribId=231&sessionId=65&materialId=poster&confId=30248).
 - [16] A. Cruz (CDF), Ph.D Thesis, University of Florida (2005).
 - [17] H. Caines (for STAR) arXiv:1012.5008 (2010).
 - [18] J. Bielcikova (for STAR), poster at this conference, [http://indico.cern.ch/materialDisplay.py?contribId=407 &sessionId=65&materialId=poster&confId=30248](http://indico.cern.ch/materialDisplay.py?contribId=407&sessionId=65&materialId=poster&confId=30248).
 - [19] Y.-s. :Lai (for PHENIX) arXiv:0911.3399. Proceedings of DPF09, eConf C090726 (2009).
 - [20] J. Putschke (for STAR) Eur. Phys. J. C61:629 (2009).
 - [21] M. Tannenbaum, Phys. Lett. B **498**, 29 (2001).
 - [22] N. Armesto, L. Cunqueiro, and C. A. Salgado, arXiv:0907.1014 [hep-ph] (2009).
 - [23] G. de Barros (for STAR) arXiv:1109.4386. (2011).
 - [24] M. Cacciari, G. P. Salam, and G. Soyez, JHEP 04, 63 (2008).
 - [25] M. Ploskon (for STAR) Nucl. Phys. A 830, 255c (2009).
 - [26] E. Bruna (for STAR) Nucl. Phys. A 830, 267c (2009).
 - [27] Y.-s. :Lai (for PHENIX) Nucl. Phys. A 830 251 (2009).
 - [28] A. Ohlson (for STAR), arXiv:1106.6243 (2011).
 - [29] M. Connors (for PHENIX) Nucl. Phys. A 855 335 (2011).
 - [30] W. Braunschweig *et al.* (TASSO), Z. Phys. C47, 187 (1990).
 - [31] N. Borghini and U.A. Wiedemann arXiv:hep-ph/0506218 (2005).
 - [32] A. Adare *et. al.*, Phys. Rev. D82, 072001 (2010).